Research paper

Ultrasound-mediated nanoparticle delivery across *ex vivo* bovine retina after intravitreal injection

Di Huang, Ying-Shan Chen, Ilva D. Rupenthal

PII: S0939-6411(17)30432-0
DOI: http://dx.doi.org/10.1016/j.ejpb.2017.06.009
Reference: EJPB 12535

To appear in: *European Journal of Pharmaceutics and Biopharmaceutics*

Received Date: 6 April 2017
Revised Date: 6 June 2017
Accepted Date: 7 June 2017

Please cite this article as: D. Huang, Y-S. Chen, I.D. Rupenthal, Ultrasound-mediated nanoparticle delivery across *ex vivo* bovine retina after intravitreal injection, *European Journal of Pharmaceutics and Biopharmaceutics* (2017), doi: http://dx.doi.org/10.1016/j.ejpb.2017.06.009

Ultrasound-mediated nanoparticle delivery across *ex vivo* bovine retina after intravitreal injection

Di Huang[1], Ying-Shan Chen[1], Ilva D. Rupenthal[1*]

[1]Buchanan Ocular Therapeutics Unit, Department of Ophthalmology, New Zealand National Eye Centre, Faculty of Medical and Health Sciences, The University of Auckland, Private Bag 92019, Auckland 1142, New Zealand

[*]Corresponding author. Tel.: +64 9 9236386; Fax: +64 9 3677173. E-mail address: i.rupenthal@auckland.ac.nz (I.D. Rupenthal).

Abstract

Intravitreal injection is the most common administration route for the treatment of retinal diseases. However, the vitreous and some of the retinal layers themselves act as significant barriers to efficient delivery of drugs administered intravitreally. This study aimed to improve the diffusive mobility of nanoparticles (NPs) in the vitreous and enhance their permeation across the retina after intravitreal injection by application of ultrasound (US). *Ex vivo* posterior bovine eye cups were used and the vitreous was either left intact or removed gently from the neural retina. Hyaluronic acid coated human serum albumin NPs were administered into the eye cups and continuous US with a frequency of 1 MHz, an intensity of 0.5 W/cm^2, and a duration of 30 s was applied once or repeatedly via the transscleral route. After pre-determined time points, fluorescence intensities in the vitreous and the retina were analyzed. Short pulses of US significantly improved the diffusive mobility of NPs through the vitreous as well as their penetration across the neural retina into the retinal pigment epithelium and choroid without causing any detectable damage to the ocular tissues. Therefore, transscleral US could be a powerful and safe tool to enhance retinal delivery of intravitreally injected NPs.

Keywords

Ultrasound; Nanoparticles; Ocular drug delivery; Retinal penetration; Intravitreal mobility; Safety

Highlights

- Ultrasound enhanced nanoparticle penetration across the retina
- Ultrasound improved the diffusive mobility of nanoparticles in the vitreous
- Ultrasound did not cause any detectable damage to the ocular tissues

Abbreviations

AMD, age-related macular degeneration; Cx43 MP, connexin43 mimetic peptide; DLS, dynamic light scattering; DPX, Distrene, Plasticizer and Xylene; DR, diabetic retinopathy; EDC, *N*-(3-dimethylaminopropyl)-*N*′-ethylcarbodiimide hydrochloride; FDA, Food and Drug Administration; FITC, fluorescein isothiocyanate; GCL, ganglion cell layer; HA, hyaluronic acid; H&E, hematoxylin and eosin; HSA, human serum albumin; ILM, inner limiting membrane; INL, inner nuclear layer; IPL, inner plexiform layer; NPs, nanoparticles; O.C.T., optimal cutting temperature; OLM, outer limiting membrane; ONL, outer nuclear layer; OPL, outer plexiform layer; PBS, phosphate buffered saline; PCL, poly(caprolactone); PdI, polydispersity index; PLGA, poly(lactide-co-glycolide); RPE, retinal pigment epithelium; TEM, transmission electron microscopy; US, ultrasound

Graphical abstract

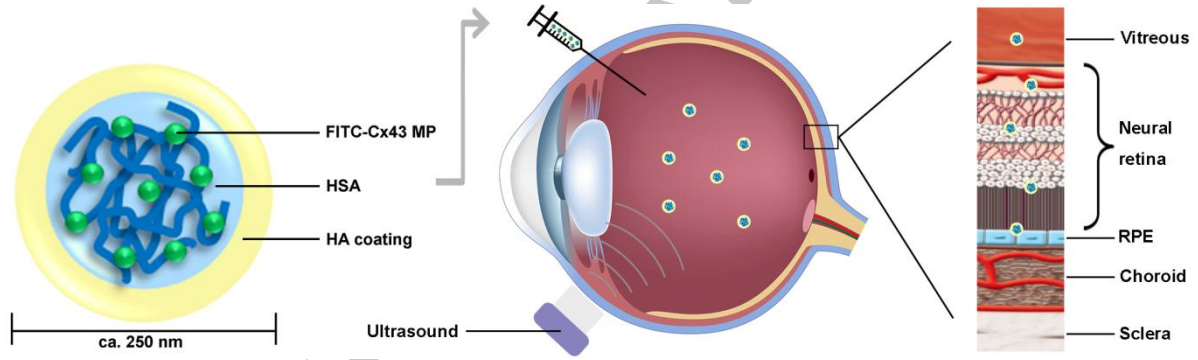

1. Introduction

Despite the great advances made in ocular drug delivery over the past decades, delivery to the retina remains challenging due to the long diffusion distance from the administration site, ocular clearance mechanisms, and the presence of various penetration barriers, especially when aiming to deliver peptides and proteins with short half-lives (minutes to hours) [1-3]. Currently, intravitreal injection is the most common and effective administration route for the treatment of retinal disorders. However, efficient targeting of specific retinal layers affected in posterior segment diseases such as age-related macular degeneration (AMD), diabetic retinopathy (DR), and glaucoma, is limited. As a result, frequent injections are required which increase the potential of unwanted side effects including retinal detachment, cataract formation, vitreous hemorrhage, and endophthalmitis [4]. Therefore, there is a clear and urgent need to develop more efficient strategies to overcome these barriers and enhance drug delivery to the target site while reducing the frequency of injection.

Nanoparticles (NPs) constitute a versatile drug delivery platform with the ability to protect their cargo from degradation, sustain drug release, penetrate physiological barriers, and deliver the drug to specific cells by either passive or active targeting mechanisms [5]. Biodegradable NPs hold significant promise for ocular drug delivery and numerous natural and synthetic biocompatible polymers such as chitosan [6], poly(lactide-co-glycolide) (PLGA) [7], and poly(caprolactone) (PCL) [8] have been evaluated *in vitro* and *in vivo* in order to enhance drug delivery efficacy. Hyaluronic acid (HA), a high molecular weight linear glycosaminoglycan composed of repeating disaccharide units of β-1,4-D-glucuronic acid-β-1,3-N-acetyl-D-glucosamine, is an important extracellular matrix component and specifically binds to several cell surface receptors, including CD44 [9]. HA modified delivery systems intended for intravitreal administration have previously been developed to enhance drug accumulation in highly CD44-expressing retinal pigment epithelium (RPE) cells and have exhibited superior cellular uptake performance via HA-CD44 receptor-mediated interactions [10, 11]. Utilizing HA modified NPs is therefore a promising strategy for targeted retinal drug delivery. However, NPs still have to diffuse through the vitreous and penetrate across the neural retina before reaching the RPE layer. After intravitreal injection, the dense vitreous network might immobilize NPs while tight junctional structures between neural retinal cells could hinder NP penetration towards the RPE, thereby limiting NP delivery efficacy.

Ultrasound (US), which is routinely used for diagnostic imaging and therapeutic applications, is currently being adopted for drug delivery purposes by transiently disrupting biomembranes. It is commonly believed that the mechanisms of US-mediated biomembrane alterations include non-thermal (e.g. cavitation, acoustic streaming, and mechanical stress) and thermal effects. In ocular drug delivery, transcorneal US has primarily been investigated to improve drug transport across the corneal epithelium [12]. However, with the development of advanced topical formulations that can more easily penetrate the cornea, this strategy is rarely being studied today. Nevertheless, other US application routes may still be of interest, especially when aiming to enhance drug delivery to the retina. Suen et al. [13] performed preliminary US studies to enhance drug delivery via the transscleral route; however, the drug reservoir which contained the aqueous protein solutions had to be in constant contact with the scleral US application site. Moreover, the actual drug concentrations reaching the retina were very low and rather unpredictable. In addition, free protein drugs may degrade rapidly while frequent US treatment may cause unwanted side effects due to a possible temperature increase in the eye. Recently, US-mediated gene delivery to the retina has been reported by Peeters et al. [14] where the US probe was directly in contact with the neural retina significantly improving retinal permeability of the gene; however, slight damage to the retinal tissues was also observed. Ultimately, applying US intravitreally even using a needle-sized probe would be rather invasive in a clinical setting and could thus cause more damage than benefits.

In the present study, transscleral US was utilized to enhance the vitreous diffusivity and retinal permeability of intravitreally administered NPs in order to achieve higher retinal drug concentrations. Connexin43 mimetic peptide (Cx43 MP), a potential therapeutic agent for the treatment of various retinal inflammatory diseases [15], was encapsulated into HA coated human serum albumin (HSA) NPs and the physiochemical characteristics of HA coated Cx43 MP HSA NPs were evaluated as described previously [16]. *Ex vivo* models using freshly collected bovine eyes were subsequently used to investigate the diffusivity of NPs in the vitreous as well as NP permeation across the retina without and with US application. Finally, histological examination and measurement of ocular surface temperature were performed to analyze if currently employed US parameters caused any damage to the ocular tissues. Overall, this work aimed to provide an initial assessment of the feasibility and safety of nanocarriers combined with US application for efficient retinal drug delivery after intravitreal injection.

2. Materials and methods

2.1. Materials

HSA (MW 66 kDa), phosphate buffered saline (PBS), 50% aqueous glutaraldehyde, *N*-(3-dimethylaminopropyl)-*N′*-ethylcarbodiimide hydrochloride (EDC), and Triton® X-100 were purchased from Sigma (St. Louis, MO, USA). Fluorescein isothiocyanate-labelled Cx43 MP (FITC-Cx43 MP, FITC-AVDCFLSRPTEKT, MW 1856 g/mol) was purchased from Auspep Pty Ltd (Tullamarine, VIC, Australia). HA (MW 120 kDa) was purchased from Lifecore Biomedical LLC (Chicago, IL, USA). Hematoxylin (Gill II) and eosin (Eosin Y) were obtained from Surgipath®, Leica Biosystems GmbH (Wetzlar, Germany). Xylene and ethanol used for histological examination were purchased from Thermo Fisher Scientific Inc. (Auckland, New Zealand). Lithium carbonate and DPX (Distrene, Plasticiser, Xylene) were from BDH Chemicals (Poole, UK). Sirius Red F3BA was purchased from Pfaltz & Bauer Inc. (Waterbury, CT, USA). Water used was pre-treated with a Milli-Q water purification system (Millipore, Billerica, MA, USA). All other commercially available chemicals were used at analytical grade. All samples were light-protected until fluorescence measurements were performed.

2.2. US device

A Sonopuls 190 device (Enraf-Nonius B.V., Rotterdam, Netherlands) equipped with a digital signal processing system software, offering an innovative method for clinical physiotherapy in a standardized and stationary manner, was utilized for these studies. The applicator was a hand-held assembly with a sound head area of 0.8 cm^2 providing ultrasonic energy with a frequency of 1 or 3 MHz. US power delivered to the target tissue was expressed in terms of the total power in watts (W) or the effective power in the radiating area of the sound head (surface intensity) in W/cm^2.

2.3. Preparation and characterization of HA coated NPs

FITC-Cx43 MP loaded HSA NPs (FITC-Cx43 MP HSA NPs) were prepared by a previously described desolvation technique [16]. Briefly, FITC-Cx43 MP was mixed with a HSA solution at 5% m_{Drug}/m_{Matrix} for 24 h at room temperature. A volume of 2.4 mL of ethanol was added dropwise to the mixture under stirring at 250 rpm for 1 h. FITC-Cx43 MP HSA NPs were then stabilized with 0.4 µL of 50% glutaraldehyde at room temperature under stirring for 24 h. Unbound FITC-Cx43 MP and FITC-Cx43 MP HSA NPs were separated by repeated washing with Milli-Q water and centrifugation at 13,000 rpm for 50 min at 4 °C (Centrifuges 5430 R, Eppendorf, Hamburg, Germany). Subsequently, surface modification of FITC-Cx43 MP HSA NPs was performed to achieve HA coating [17]. HA was initially dissolved in 0.1 M sodium acetate buffer pH 4.5 to a final concentration of 2 mg/mL and pre-activated by incubation with *N*-(3-dimethylaminopropyl)-*N'*-ethylcarbodiimide hydrochloride (EDC) for 2 h at 37 °C. The activated HA was then added to a suspension of FITC-Cx43 MP HSA NPs, buffered by 0.1 M borate buffer to pH 9, and incubated overnight at 37 °C. The resulting HA coated FITC-Cx43 MP HSA NPs were purified by centrifugation as previously mentioned and re-suspended in Milli-Q water using an ultrasonic processor (UP 200S, Hielscher, Teltow, Germany) at an amplitude of 40% and a duty cycle of 0.4 s for 1 min on an ice bath.

Particle size, distribution, and zeta potential were determined by dynamic light scattering (DLS) using a Malvern Nano ZS (Malvern Instruments, Worcestershire, UK), and the mean value as well as the standard deviation of three different batches were recorded. Morphological observation of HA coated FITC-Cx43 MP HSA NPs was performed by transmission electron microscopy (TEM) using a Tecnai^{TM} G^2 Spirit Twin TEM (FEI Company, Hillsboro, OR, USA) at an accelerating voltage of 120 kV.

2.4. US-enhanced NP penetration across the retina

2.4.1. Experimental procedure

Fresh bovine eyes were obtained from a local abattoir and used within 3 h. Eyes were treated as previously described by Pitkanen et al. [18]. Briefly, after removal of extraocular tissues, an incision through the sclera on the side of the eyeball around 8-10 mm behind the limbus was made using a blade and the initial incision was circumferentially extended around the entire eye using scissors. The anterior segment and vitreous were separated gently from the neural retina. The obtained posterior eye cups were placed into the wells of a six-well plate and 1 mL of HA coated NPs with a final FITC-Cx43 MP concentration of 20 µM was added onto the neural retina inside the eye cups. Subsequently, US of continuous wave (100% duty cycle) was applied either intravitreally or transsclerally with a frequency of 1 MHz, an intensity of 0.5 W/cm^2, and a short duration of 30 s with the experimental set-

up schematically depicted in Fig. 1. After US application and 4 h of incubation with NP suspensions at 37 °C, all treatments were removed from the eye cups and the surface of the neural retina was gently washed three times with PBS. Neural retina and retinal pigment epithelium (RPE)/choroid complex were carefully peeled off from the eye cups, collected, and weighed. Tissue samples were then homogenized on an ice bath in 500 µL of PBS containing 2% Triton® X-100. After centrifugation at 5,000 rpm for 20 min at 4 °C, supernatants were collected and the drug concentration was determined via fluorescence at an excitation and emission wavelength of 488 and 528 nm, respectively, using a fluorescence microplate reader (Synergy 2, BioTek Instruments, Winooski, VT, USA). Fluorescence intensities in the neural retina and the RPE/choroid were expressed per gram of tissue after subtraction of any background fluorescence from blank tissues without any treatment.

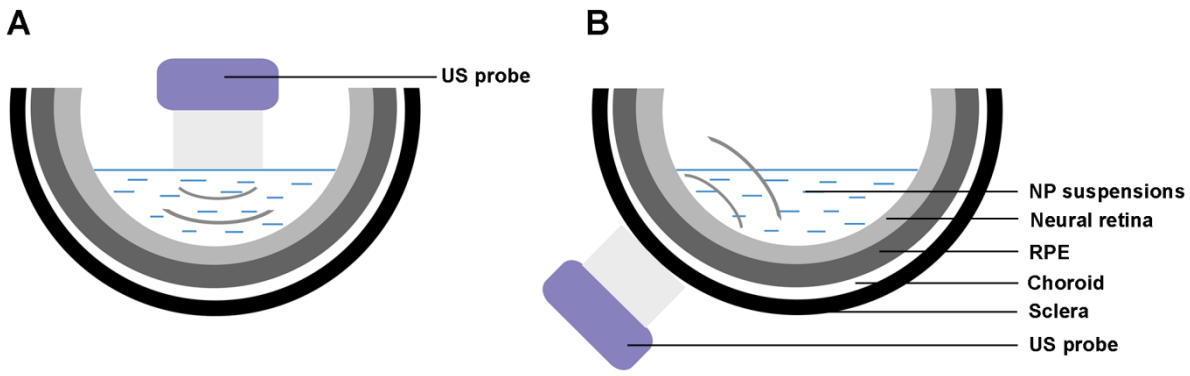

Fig. 1. Experimental set-up of NP penetration studies with US application using bovine eye cups *ex vivo* adapted from Peeters et al. [14]. (A) Intravitreal US: US probe was in direct contact with the surface of the NP suspension inside the eye cup. (B) Transscleral US: US probe was positioned onto the sclera outside the eye cup.

2.4.2. Intravitreal US

2.4.2.1. Effect of US duration on NP penetration

The general procedure used here is described in section 2.4.1. US applied directly onto the surface of the NP suspension inside the eye cups was defined as intravitreal US (Fig. 1A) and was used in this series of experiments. A volume of 1 mL of NP suspension was added to the eye cups after which US was administered for 30 or 120 s, respectively. Eye cups were subsequently incubated for 4 h before assessment. A passive NP permeation group without US application was also included.

2.4.2.2. Effect of time lapse on US-enhanced NP penetration

To verify that the effect of US-enhanced NP penetration was temporary, eye cups containing 1 mL of PBS were initially subjected to US treatment and incubated for 15 min. Subsequently, PBS was

removed and replaced with 1 mL of the NP suspension which was then incubated for another 4 h. The result from this experiment were compared to that of passive NP permeation after 4 h.

2.4.2.3. Reproducibility of US-enhanced NP penetration

Eye cups containing 1 mL of PBS were subjected to 30 s of US. After incubation for 15 min, PBS was removed and replaced with 1 mL of NP suspension, with US of the same setting applied again before incubation of the eye cup for another 4 h. The result from this experiment was compared to that of eye cups incubated with the NP suspension for 4 h after a single US treatment of 30 s.

2.4.2.4. Repeatability of US-enhanced NP penetration

To compare the influences of single and repeated US application on enhanced NP permeation across the retinal tissues, eye cups were firstly incubated with 1 mL of NP suspension and then subjected to one 30 s US treatment. Following 15 min of incubation, US was applied again. The 15 min incubation time followed by 30 s of US application was performed up to three times prior to incubation for 4 h.

2.4.3. Transscleral US

The general procedure used here is described in section 2.4.1. US applied to the sclera outside of the eye cups was defined as transscleral US (Fig. 1B) and was used in this set of experiments. Similar to intravitreal US, repeated transscleral US application consisted of two steps. Firstly, 1 mL of NP suspension was added to the eye cups after which 30 s of US was administered via the transscleral route. Secondly, eye cups were incubated for 15 min. Steps one and two were repeated up to a total of three cycles followed by tissue incubation for 4 h. To further investigate the effects of different US application routes (i.e. transscleral and intravitreal US) on the enhancement of US-mediated NP penetration across the retina, results from this experiment were compared to those of eye cups incubated with NP suspensions for 4 h with triple application of 30 s intravitreal US.

2.5. Tracking NP diffusion in the vitreous

The vitreous gel is inherently fragile and liquefaction occurs quickly after removal from the eye. Thus, as the microstructure of the vitreous can be easily disrupted by gravitational force without ocular support, an intact *ex vivo* vitreous model using the eye cup was used to reduce any damage to vitreous integrity and mimic NP diffusion after intravitreal injection *in vivo*. Bovine eyes were treated similarly to the procedure described in section 2.4.1. After removal of the anterior segment of the eye, 20 μL of HA coated NP suspension with a final FITC-Cx43 MP concentration of 200 μM was gently injected into the intact vitreous at an approximately 5 mm depth using a syringe with a 30G needle. For each bovine eye, only one condition was tested. Whatman™ lens cleaning tissues were used to gently remove any excess liquid on the vitreous surface generated during eye dissection and NP

injection. A Burton lamp (G. Nissel & Co. Ltd., London, UK) was placed over the eye cup to illuminate the fluorescent NPs and assist visualization of NP diffusion in the vitreous. Images were recorded immediately after NP injection (baseline). Transscleral US of 30 s was then applied three times with a 1 min wait time in-between. An additional set of images was then recorded 5 min post-NP injection. Intravitreally administered NPs, diffusing passively in the vitreous without US application, were used as a control. Fluorescence areas and intensities immediately after NP injection and after 5 min of diffusion were quantified using ImageJ software and the fold change was calculated by dividing values after 5 min by the results obtained immediately after injection.

2.6. Quantitative analysis of NP distribution in the vitreous

Whole porcine eyes were used to quantitatively analyze NP distribution in the vitreous without and with US application. The experimental set-up is schematically shown in Fig. 2. Briefly, after removal of extraocular tissues and washing with PBS to remove any blood from the ocular surface, eyes were placed into the wells of a 12-well plate. Subsequently, each eye was intravitreally injected through the pars plana with 20 µL of HA coated NP suspension with a final FITC-Cx43 MP concentration of 200 µM using a syringe with a 30G needle at an angle of 15-30 °. Eyes were then transferred into a water bath at 37 °C for US treatment and further incubation (Fig. 2A and 2B). The US transducer probe was positioned directly onto the sclera adjacent the equator and triple US of 30 s with a wait time of 15 min was applied. The region of US application was labeled with a marker. One hour after injection, porcine eyes were snap-frozen in liquid nitrogen and dissected into two equal parts along the visual axis of the eye (Fig. 2C). After removal of any attached retinal tissue, the vitreous of both the injection and non-injection side was carefully collected, weighed, and homogenized. Homogenates were centrifuged at 4,500 rpm for 5 min at 4 °C. Supernatants were collected and the amount of particles present in each half was measured using a microplate reader. The fluorescence intensity in each half of the vitreous was expressed per gram of vitreous after subtraction of any background fluorescence obtained from blank homogenized vitreous without treatment.

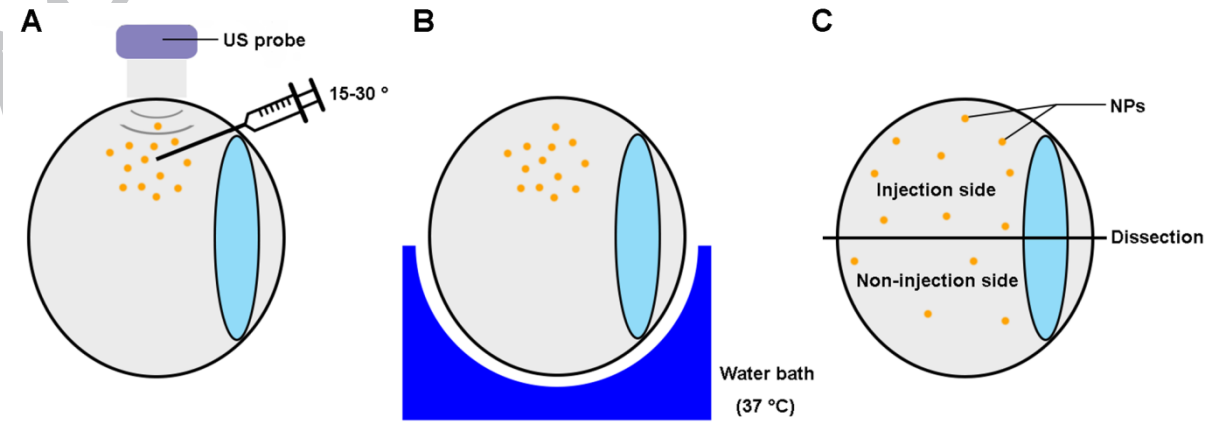

Fig. 2. Set-up for quantitative analysis of NP distribution in the vitreous using whole porcine eyes *ex vivo*. (A) NP suspensions were intravitreally injected and triple 30 s US was applied directly onto the sclera near the equator. (B) Eyes were kept in a water bath at 37 °C after NP injection and US treatment. (C) The vitreous was collected from both the injection and the non-injection side and the fluorescence intensity in each part was analyzed after dissection.

2.7. Histological examination

Fresh bovine eyes were treated with triple 30 s transscleral US as described above. The region of US application was labeled with a marker, cut into small pieces (20 × 15 mm), immersed in optimal cutting temperature (O.C.T.) compound (ProSciTech, Sydney, Australia), and snap-frozen with liquid nitrogen. Cross-sections of 10 µm thickness were cut using a cryostat microtome (CryoStar^{TM} NX50, Thermo Scientific, Waltham, MA, USA) and were mounted onto adhesive slides before performing hematoxylin and eosin (H&E) staining for histological visualization. Briefly, sections were immersed in tap water for 5 min to remove any O.C.T. followed by staining with hematoxylin for 5 min. After differentiating in 1% acid alcohol for two dips and rinsing in tap water, slides were dipped in lithium carbonate solution until sections turned blue. Afterwards, slides were rinsed under tap water and stained with 1% eosin for ten dips. Finally, sections were dehydrated using absolute ethanol, cleared by xylene, and mounted in DPX mounting medium. All stained sections were imaged at 5× (scleral sections) and 10× (retinal/choroidal sections) magnification using a Leica DMRA HC fluorescence microscope (Leica Microsystems, Wetzlar, Germany) coupled with a digital camera (DS-5MC, Nikon, Tokyo, Japan) and images were processed using the NIS-Elements BR 4.30.00 64-bit imaging software (Nikon, Tokyo, Japan).

To further analyze the scleral collagen arrangement, 10 µm thickness scleral sections (parallel to the ocular surface) were cut and stained for 1 h with 0.1% Sirius Red in saturated aqueous picric acid for collagen bundle staining. US of 30 s was applied on top of the coverslip with US contact-gel added in between. Afterwards, sections were immediately observed at 10× and 20× magnification under a polarized light microscope (Leica Microsystems, Wetzlar, Germany) and images were processed using Leica Application Suite software version 4.3 (Leica Microsystems, Wetzlar, Germany). The same area was imaged before and after US application, with application of US generated by an ultrasonic processor at an amplitude of 80% and a duty cycle of 0.8 s for 1 min at room temperature used as a positive control.

2.8. Temperature alterations

To account for any potential thermal damage, heat maps of the ocular surface before and after 30 s of US application (1 MHz, 0.5 W/cm2) were recorded at room temperature using an infrared thermography system TVS-200EX (NEC Avio Infrared Technologies Co., Tokyo, Japan) with scleral

temperature alterations at the site of US application analyzed using Goratec Thermography Studio Software version 4.8 (Goratec Technology, Erding, Germany). A positive control was performed by applying 30 s of US with a higher intensity (1 MHz, 2 W/cm2).

2.9. Statistical analysis

All studies were performed in triplicate and data points were expressed as mean values plus or minus standard deviation (mean ± S.D.). To determine statistical significance, analysis of variance (two-way ANOVA) followed by Tukey's multiple comparison was performed using GraphPad Prism 7. Differences were considered statistically significant if $p \leq 0.05$.

3. Results and discussion

3.1. Characterization of HA coated NPs

HA coated FITC-Cx43 MP HSA NPs were successfully prepared by the desolvation technique followed by HA surface coating via an EDC reaction. A schematic morphological illustration of HA coated FITC-Cx43 MP HSA NPs is shown in Fig. 3A. HA coated FITC-Cx43 MP HSA NPs were expected to possess a core-shell structure with FITC-Cx43 MP encapsulated into the HSA matrix surrounded by an outer HA coating layer. Results obtained by DLS showed that HA coated FITC-Cx43 MP HSA NPs possessed a particle size of 252.70 ± 7.29 nm and a relatively narrow size distribution with a polydispersity index (PdI) of 0.07 ± 0.03 (Fig. 3C). The zeta potential was in the range of -43.97 ± 0.38 mV preventing particle aggregation in suspension. A number of studies have extensively investigated the effect of particle size and surface characteristics (e.g. charge and concentration) on the vitreous mobility of NPs with hydrophobic, electrostatic, and steric effects significantly contributing to NP diffusion [19, 20]. Specifically, NPs with a particle size larger than 1000 nm are generally immobilized in the vitreous due to steric hindrance, highly concentrated NPs in suspensions aggregate in the vitreous due to hydrophobic effects, and positively charged NPs bind to the negatively charged vitreous meshwork thus being retained. Therefore, the highly negative surface charge and the relatively small particle size of HA coated FITC-Cx43 MP HSA NPs render them a promising nano-sized drug delivery platform for intravitreal administration.

The morphology of HA coated FITC-Cx43 MP HSA NPs was examined by TEM. Particles demonstrated a spherical shape with a size of around 250 nm, exhibiting a dark core surrounded by a lighter gray rim (Fig. 3B) suggesting a drug-containing HSA matrix coated by HA. Thus, the TEM image further supported the results obtained by DLS and confirmed successful HA coating onto the surface of FITC-Cx43 MP HSA NPs.

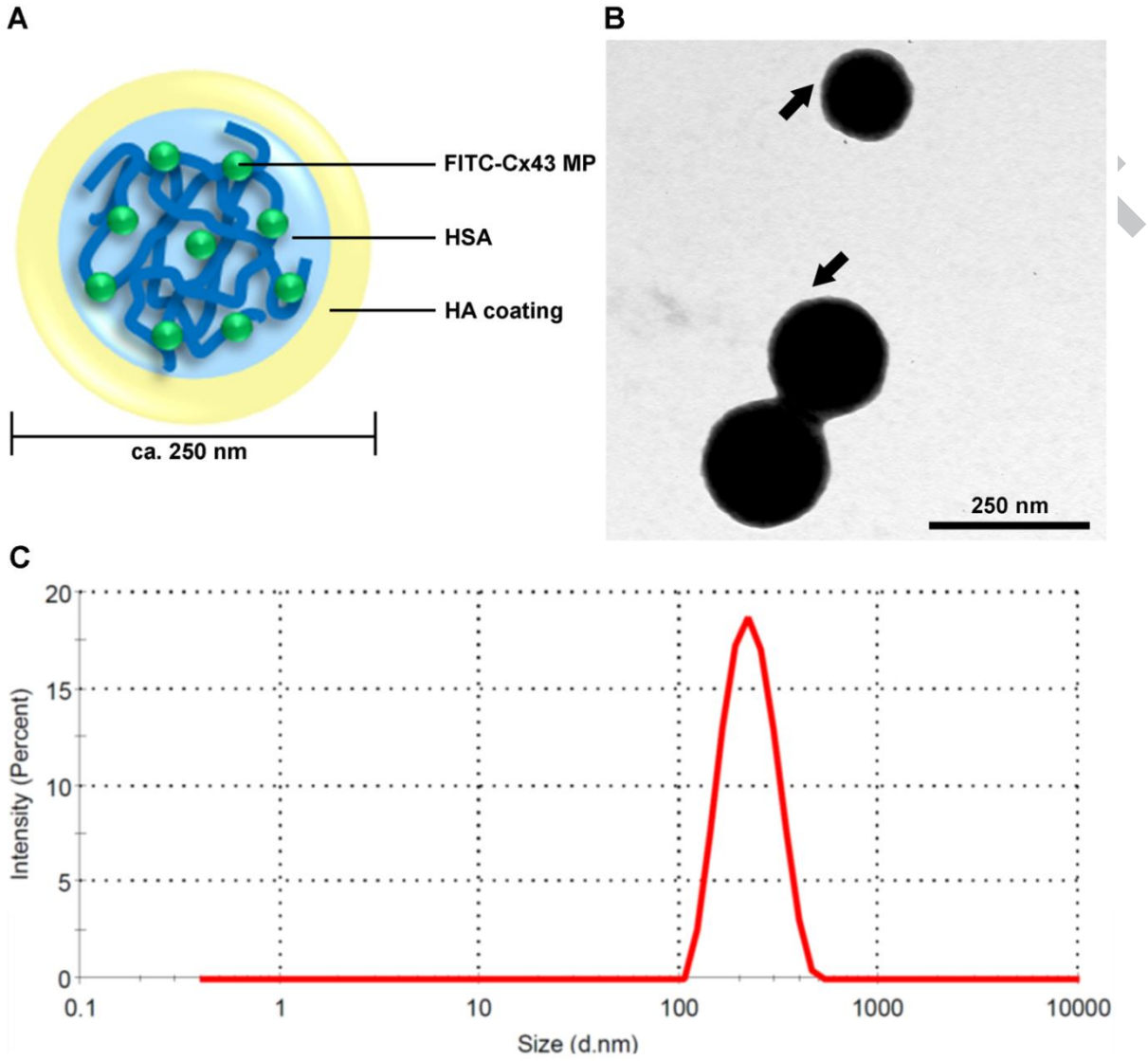

Fig. 3. Physicochemical characteristics of HA coated FITC-Cx43 MP HSA NPs. (A) Schematic illustration of HA coated FITC-Cx43 MP HSA NPs, comprising a core-shell structure with a particle size of approximately 250 nm. (B) TEM image of HA coated FITC-Cx43 MP HSA NPs with black arrows marking the lighter coloured HA coating [21]. (C) Sample size distribution of HA coated FITC-Cx43 MP HSA NPs measured by DLS.

3.2. Intravitreal US-enhanced NP penetration across the retina

Fig. 4A compares NP penetration across the retina without and with intravitreal US application. In the absence of US, only very few NPs penetrated across the neural retina and into the RPE/choroid after 4 h of passive diffusion, whereas brief US application (1 MHz, 0.5 W/cm^2, 30 s) led to a significant increase ($p \leq 0.05$). However, extending the duration of a single US application from 30 to 120 s did not result in any further NP penetration into neural retina or RPE/choroid ($p > 0.05$), suggesting that the US-mediated penetration enhancement is transient and might have already reached its maximum

threshold after a short US pulse. The neural retina is known to form a strict permeation barrier even for nano-sized drug delivery systems due to the presence of the inner limiting membrane and the inter-photoreceptor matrix, which significantly block drug and particle transport [22]. Previous research demonstrated that US acted as a powerful tool to transiently increase the permeability of ocular tissues and concluded that US-induced cavitation was the primary mechanism with the presence of bubble activities enhancing ocular drug delivery [14, 23-25]. In our experiment, an US intensity of 0.5 W/cm^2 was selected to produce sufficient acoustic pressure to generate oscillating bubbles and induce microstreaming which can reversibly change the lipid bilayer, create aqueous pathways, and result in decreased resistance to the transport of macromolecules [26]. The corresponding shear stress and surface divergence could also contribute to the improvement of retinal permeability by disrupting tight cell membrane barriers [27, 28].

As there appeared to be a temporary window after sonication during which the retinal permeability of NPs remained elevated, the effect of time lapse on intravitreal US-mediated permeation improvement was investigated. The neural retina was firstly treated with US for 30 s and incubated with PBS only (without fluorescent NPs) for 15 min before application of the NP suspension. As shown in Fig. 4B, no significant particle penetration improvement was observed between the passive diffusion (no US) and the US-treated group ($p > 0.05$), when particles were not present at the time of US application. This result suggests that retinal permeability only increased during or shortly after sonication, highlighting that membrane disruption is only transient with no permanent tissue damage expected. Moreover, it suggests that applied drugs or NPs need to be close to the barrier during US application in order to improve their permeability.

Fig. 4C demonstrates fluorescent NPs in both the neural retina and the RPE/choroid when intravitreal US was firstly applied to eye cups incubated with PBS only for 15 min, after which PBS was replaced by the NP suspension and US was re-applied. Intensities were comparable to the group in which US was applied only once to the neural retina incubated with the NP suspension ($p > 0.05$), suggesting that US-mediated penetration enhancement of NPs was reproducible and that previous US application had no overlapping or additive effect. This observation further supported that retinal permeability of NPs was enhanced by US-induced physical disruption of biomembranes lasting only seconds to minutes with endogenous vesicle-based healing processes resulting in fast resealing of these openings [29]. The original biological structures of tight junctions seemed to recover shortly after sonication with repeated treatment re-opening the structures thus allowing reproducible US application.

In addition to the reproducibility, the repeatability of intravitreal US-enhanced NP delivery was evaluated by applying repeated US of 30 s after a wait time of 15 min. Results shown in Fig. 4D indicate that when US was applied twice, the fluorescence intensities in the neural retina and RPE/choroid were enhanced approximately 1.20 and 1.54 times, respectively. Triple US application

resulted in a 1.34-fold increase in the fluorescence intensity in the neural retina and a 1.62-fold increase in the RPE/choroid compared to single US treatment, suggesting that repeated US application significantly improved the amount of NPs penetrated into both the neural retina ($p \leq 0.001$) and the RPE/choroid ($p \leq 0.01$) compared to single US application. It appears that while single US application using the current settings was able to transiently disrupt the barriers of the neural retina and increase retinal permeability of the NPs to a certain degree, repeated US treatment resulted in a cumulative but non-linear enhancement of NP transport. Nevertheless, more detailed studies on US-enhanced penetration of NPs are required to optimize the US settings for the clinical setting.

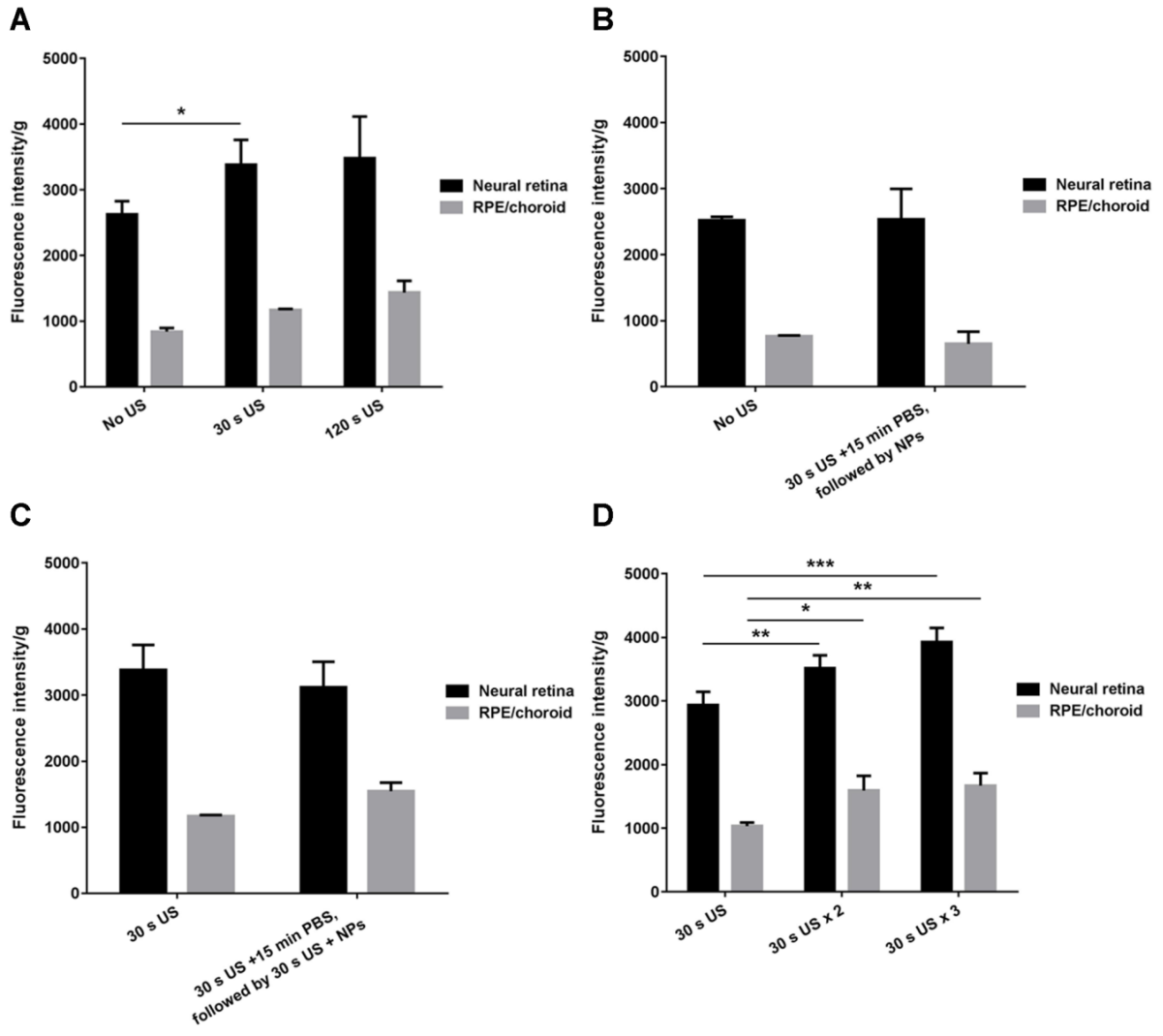

Fig. 4. Intravitreal US-enhanced NP penetration through the retina using bovine eye cups *ex vivo*. (A) Effect of US duration on retinal permeability of NPs. (B) Effect of time lapse on US-mediated enhancement. (C) Reproducibility of US-enhanced NP penetration. (D) Repeatability of US-enhanced NP penetration (data points represent mean values ± S.D., n=3).

3.3. Transscleral US-enhanced NP penetration through the retina

The effect of transscleral US-enhanced retinal NP permeability was evaluated and results were compared with those of intravitreal US application. Similarly, in the absence of transscleral US, fluorescence intensities per gram of tissue reached 2289.66 ± 37.61 and 930.19 ± 93.70 in the neural retina and RPE/choroid, respectively, solely by passive diffusion. The application of 30 s transscleral US significantly improved NP penetration to 2918.54 ± 22.17 ($p \leq 0.0001$) and 1193.87 ± 229.93 ($p \leq 0.05$) in the neural retina and RPE/choroid, respectively (Fig. 5A). In addition, triple transscleral US application led to a further 1.17-fold enhancement in fluorescence intensity both in the neural retina and the RPE/choroid compared to single US treatment, suggesting that even transsclerally applied US was able to enhance retinal permeation of NPs with repeated application further improving the amount of NPs penetrated, probably due to the same mechanisms as described above.

Fig. 5B compares the NP penetration after triple intravitreal and transscleral US application. Intravitreal US enhanced NP penetration into the neural retina to a greater extent than transscleral US ($p \leq 0.01$). One possible explanation is that the distance between the US transducer and the neural retina in transscleral US was longer than that of exposing US directly to the surface of the NP suspension sitting on the neural retina. During energy transport, other ocular tissues including the sclera and choroid might also absorb parts of the US energy thereby decreasing the actual intensity on the neural retina. In addition, the streaming direction of intravitreal US energy was outward (i.e. from the retina to the sclera) which would further facilitate NP permeation in that direction, whereas the streaming direction of transscleral US was the opposite way.

However, while intravitreal US application resulted in higher particle permeation, this technique would be rather difficult and invasive to perform in a clinical setting requiring vitreoretinal surgery to place the US transducer probe into the vitreous using a transconjunctival sutureless vitrectomy system [30]. Moreover, due to the sensitivity of the photoreceptors which send signals to the brain via the visual pathways, long-term application of intravitreal US might lead to structural or functional alterations of the retina thereby causing vision impairment or loss. On the other hand, when transscleral US is applied, any minor structural changes caused by the US energy are considered acceptable, as the sclera is a fibrous structure and is much less innervated than the retina [31]. In addition, the therapeutic target spot in the retina is generally located around 20 mm behind the site of US application on the sclera in human eyes, which could minimize damage to the retina through absorption of some of the energy while still allowing for sufficient cavitation for enhanced drug/particle permeation. Therefore, this experiment underlined the importance of keeping a good balance between efficacy and safety of the applied US.

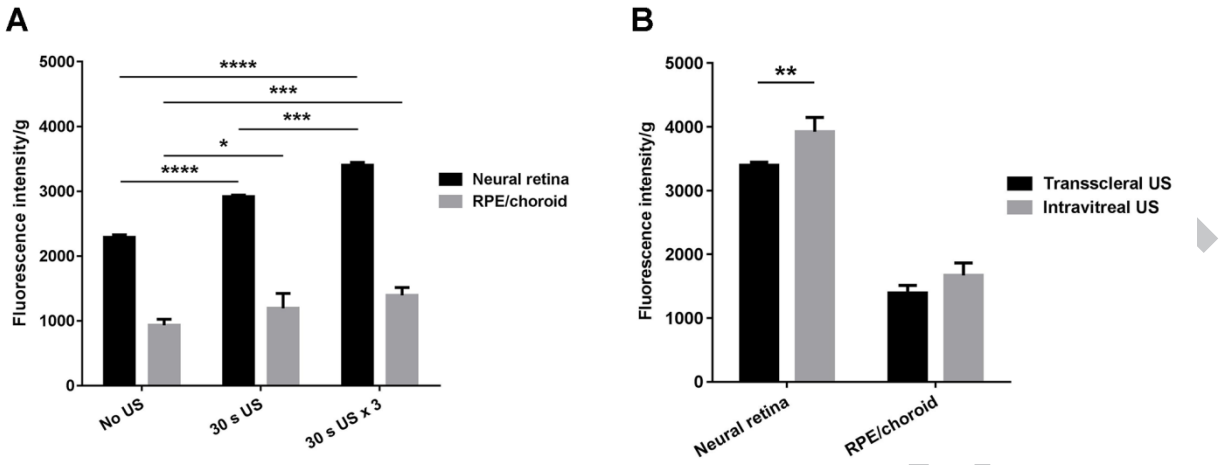

Fig. 5. Transscleral US-enhanced NP penetration through the retina using bovine eye cups *ex vivo*. (A) Repeatability of transscleral US-enhanced NP penetration. (B) Comparison of the enhancement of NP penetration across the retina after transscleral and intravitreal US application (data points represent mean values ± S.D., n=3).

3.4. Tracking NP diffusion in the vitreous

Intact bovine vitreous remaining in the posterior eye cups was utilized to evaluate the influence of transscleral US on NP mobility in the vitreous. Bovine eyes were selected in this experiment as an *ex vivo* model for mammalian vitreous, as it demonstrates a similar composition and microstructure to human vitreous [32]. Fig. 6A shows that a large amount of NPs remained at the initial injection spot after 5 min without US application likely due to interactions with the hydrophobic domains of the collagen fibrils in the vitreous. It is commonly believed that adhesive interactions between NPs and the vitreal network play an importment role in NP diffusion through the vitreous and may even overcome the electrostatic repulsion expected between negatively charged particles and vitreous constituents (i.e. glycosaminoglycans). This would slow down the movement of NPs and cause their relatively high retention at the injection site in the vitreous [19]. In contrast to the passive difussion group (no US), triple transscleral US assisted NP diffusion away from the injection site to the surrounding vitreous. Here the region of the vitreous adjacent to the injection site showed gradual spreading of NPs 5 min after injection. Moreover, a rapid increase in the distribution area as well as a decrease in the fluorescence intensity at the original injection site were observed after triple US application (Fig. 6B), suggesting that the application of transscleral US had a substantial effect on the interference of the vitreal collagen meshwork with NP diffusive mobility in the vitreous.

NP diffusion in the vitreous has important implications for targeted drug delivery to the retinal tissues. It is worth mentioning here that the vitreous has a negatively charged meshwork structure with the mesh size specifically in the central bovine vitreous being approximately 550 nm. The vitreous is a viscoelastic liquid generally allowing the diffusion of the NPs with a size smaller than the mesh pores

[19], although the charge of the particles also plays a significant role. HA coated NPs used in this study possessed suitable physicochemical characteristics including a small particle size of 252.70 ± 7.29 nm and a negative surface charge, which should avoid steric trapping within the vitreous meshwork and allow NPs to diffuse relatively freely through the vitreous via electrostatic repulsion from the negatively charged glycosaminoglycans in vitreous meshwork. Applying repeated transscleral US might also transiently disrupt the vitreous meshwork structure and increase the size of the mesh pores as well as the convective flow thereby further enhancing the diffusive mobility of NPs in the vitreous. However, further studies on the mechanisms are needed to broaden our understanding of US-enhanced particle movement in the vitreous.

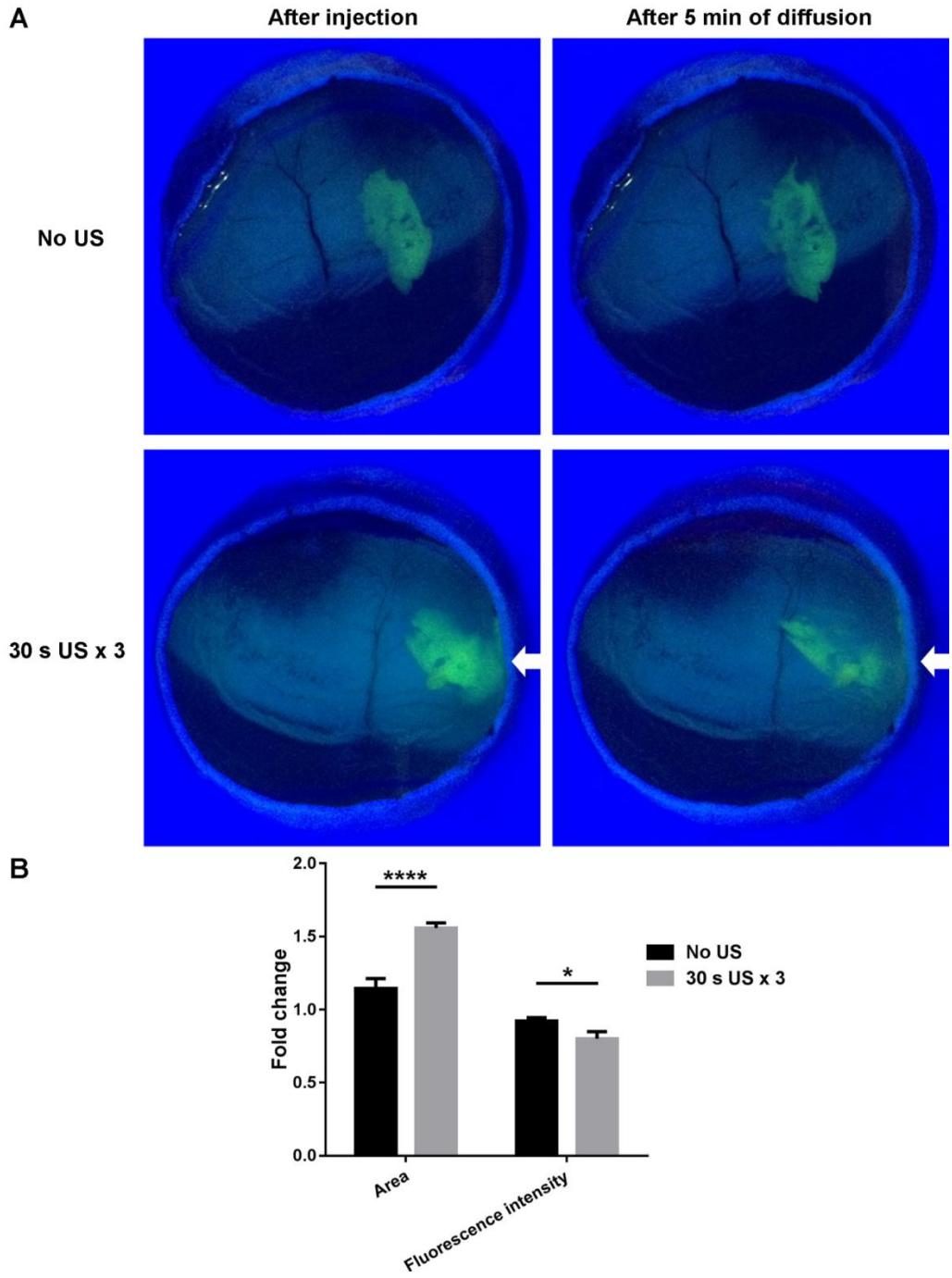

Fig. 6. NP diffusion in intact bovine vitreous *ex vivo* without or with US application. (A) NP distribution in the vitreous immediately after intravitreal injection (left) and after 5 min of diffusion (right) without (top) and with triple transscleral US application (bottom). White arrows mark the site of US application. (B) Quantification of the fold change in fluorescent area and intensity using ImageJ software (data points represent mean values ± S.D., n=3).

3.5. Quantitative analysis of NP distribution in the vitreous

To quantify the distribution of NPs in the vitreous 1 h after intravitreal injection without and with triple transscleral US application, whole porcine eyes were employed and dissected into equal two half-balls along the visual axis of the eye after being snap-frozen. Results shown in Fig. 7 demonstrate that the fluorescence intensity in the injection half was significantly higher than in the non-injection half of the passive diffusion group without US application ($p \leq 0.001$), suggesting that most of the injected NPs remained near the injection site. Compared to passive diffusion, the US-treated group exhibited a more uniform distribution of NPs throughout the whole vitreous 1 h after injection with no significant difference between the fluorescence intensities in the injection and the non-injection halves ($p > 0.05$). These results further support the hypothesis that NP movement in the vitreous could be facilitated by US energy.

While these studies investigated the effect of US application on the diffusive behaviour of intravitreally injected NPs and confirmed that transscleral US may enhance NP mobility in *ex vivo* bovine and porcine vitreous, it remains important to take the following two points for future *in vivo* studies into account. Firstly, it is known that an anterior-posterior convective flow is present in the vitreous *in vivo*, which might affect the movement of intravitreally injected NPs towards the retina as well as the rate of clearance via the aqueous outflow. Previous studies have investigated the coupled convective-diffusive delivery of drugs in the vitreous and have shown that the consideration of convective transport is particularly important in the development of controlled-release systems as convection accounts for around 30% of the total intravitreal drug transport [33, 34]. Nevertheless, it is expected that the enhanced diffusive mobility of NPs mediated by US application in the here presented *ex vivo* vitreous model will also be observed in an *in vivo* environment, where convective movement towards the posterior part of the eye might further assist retinal delivery of intravitreally injected NPs. Secondly, mammalian (i.e. bovine and porcine) vitreous was used in this *ex vivo* work, which may differ slightly from human vitreous with properties also greatly depending on the age and disease state which could also greatly influence the mobility of intravitreally injected NPs *in vivo*. Further *in vivo* studies are required especially on models with various ocular disorders such as AMD and DR, which could contribute to the optimization of US-mediated retinal delivery of nanocarriers to treat these diseases more efficiently.

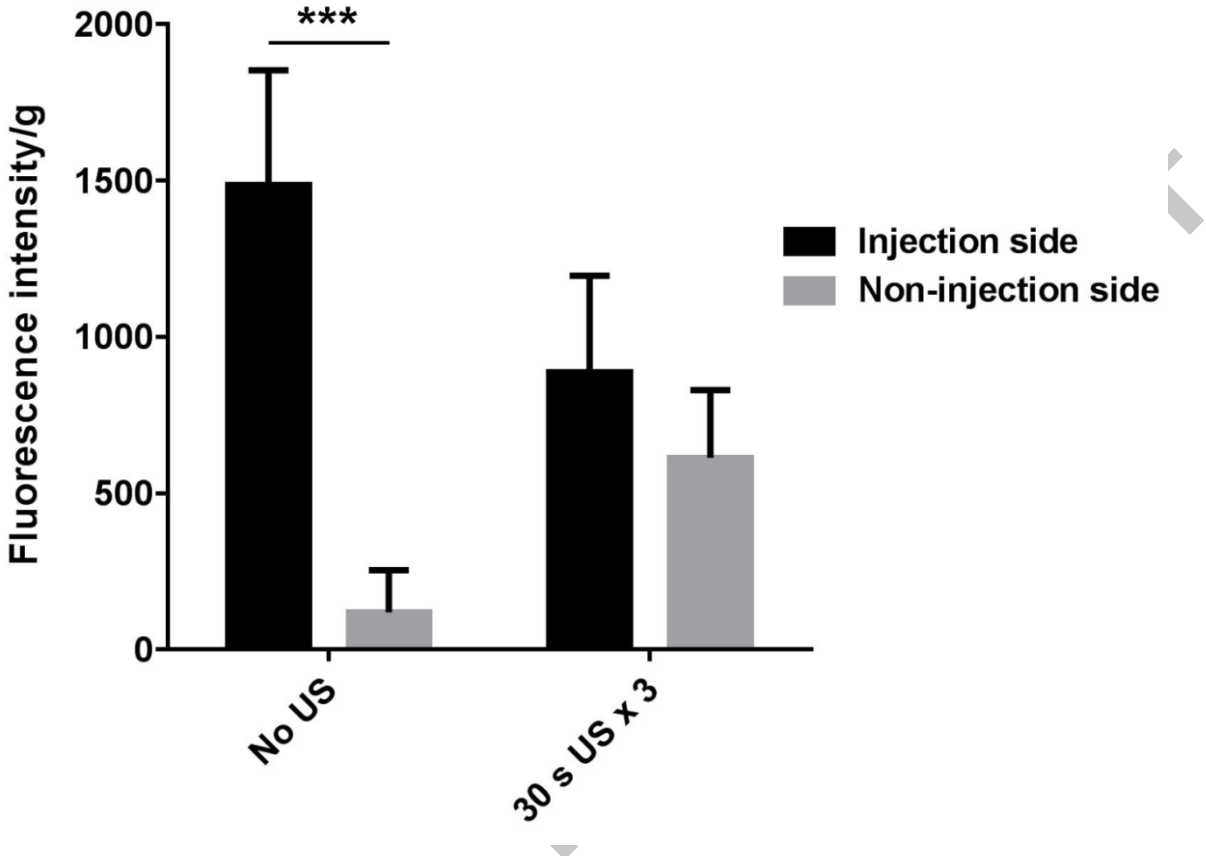

Fig. 7. Quantitative analysis of NP distribution in the vitreous of porcine eyes *ex vivo* after intravitreal injection (data points represent mean values ± S.D., n=3).

3.6. Histological examination

To assess whether US application caused any damage to the eye, sections of US-treated ocular tissues were stained with H&E, examined under a light microscope, and compared to control tissues without US application (Fig. 8). Microscopically, the overall morphological structure of the retina and other ocular tissues (including the sclera and choroid) of US-treated eyes were found unchanged when compared to control eyes without US treatment. In both groups, the integrity of the retinal layers was maintained with no obvious thinning or swelling observed, while the retinal thickness as well as the number of nuclei in each of the retinal layers also remained consistent. Fibers in scleral sections were arranged in bundles parallel to the surface, suggesting normal scleral morphology. In addition, the US treatment did not cause any retinal detachment or deformation of the retinal layers at the US application site, although it should again be noted that these results could differ slightly in an *in vivo* setting.

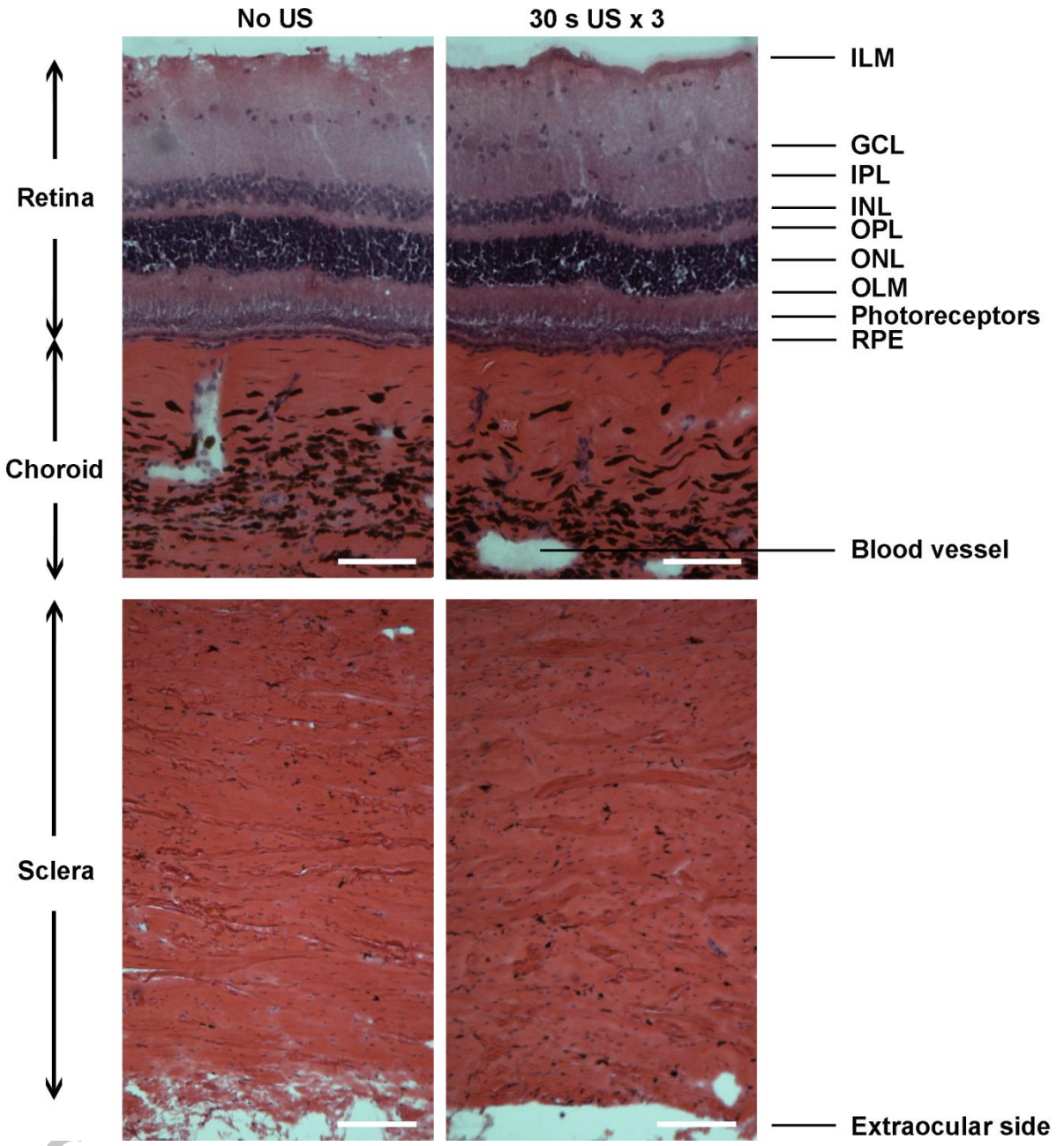

Fig. 8. H&E examination of the effect of transscleral US application on retinal/choroidal and scleral structures. Scale bar = 100 µm in retinal/choroidal sections and 200 µm in scleral sections. ILM, inner limiting membrane; GCL, ganglion cell layer; IPL, inner plexiform layer; INL, inner nuclear layer; OPL, outer plexiform layer; ONL, outer nuclear layer; OLM, outer limiting membrane and RPE, retinal pigment epithelium.

To further evaluate whether US application disrupted the collagen network in the sclera, scleral sections were stained by picrosirius red which associates with cationic collagen fibrils and enhances their natural birefringence under polarized light [35]. As shown in Fig. 9, collagen bundles in the sclera interweaved with each other to form a regular network structure with no significant alterations

in alignment orientation of collagen bundles observed without and with 30 s of US application. However, the collagen network structure in the positive control sample (high amplitude ultrasonic probe) was significantly changed, accompanied by narrowing and dissociation of the collagen bundles and a reduction in collagen fibril diameters. The interlaced structure of scleral collagen bundles is functionally important for maintaining rigidity and flexibility of the eye ball and protecting it against changes in intraocular pressure. Thus it is important to ensure that transscleral US does not permanently damage the collagen structure of the sclera.

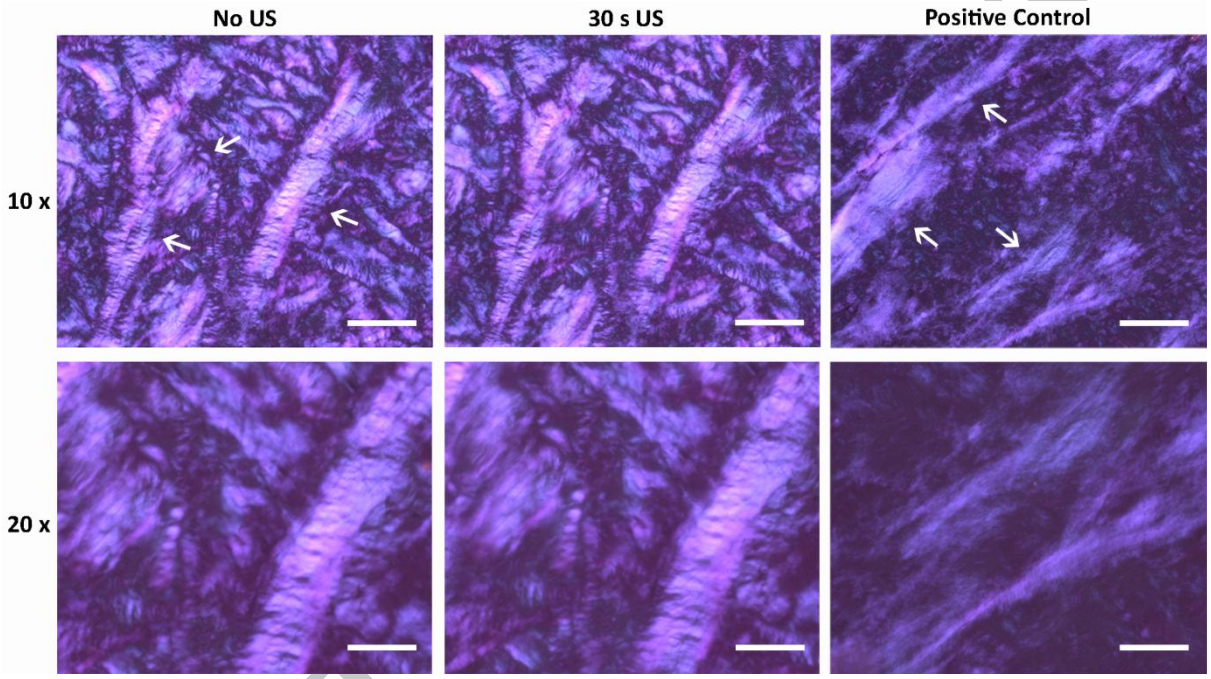

Fig. 9. Examination of scleral collagen arrangement without and after US application. Scale bar = 200 and 100 µm in the images captured at 10× and 20× magnification, respectively. White arrows mark collagen bundles in the sclera.

3.7. Temperature alterations

Temperature alterations in the eye after US application were measured by a thermographer to identify the contribution of thermal effects on particle mobility and eliminate any possible tissue damage. As shown in Fig. 10, the average temperature rise was 1.3 °C after US application under the current operating conditions, which is below the maximum limit of 1.5 °C for diagnostic US applications in ophthalmology even in the absence of blood flow. A significant temperature increase of 3.0 °C on the ocular surface was observed in the positive control sample where a higher US intensity of 2 W/cm^2 was applied. It was also noted that the temperature only changed at the US application site whereas the temperature of other tissues remained constant before and after US application, suggesting that the heat generation induced by US energy was mainly due to direct tissue contact. Therefore, the observed unchanged tissue structures of sclera and retina as well as the negligible temperature

increase suggest that US treatment using the current settings did not cause any detectable damage, although further *in vivo* studies may be required to confirm this, especially with regards to any structural and functional changes due to a possible temperature rise or mechanical stress.

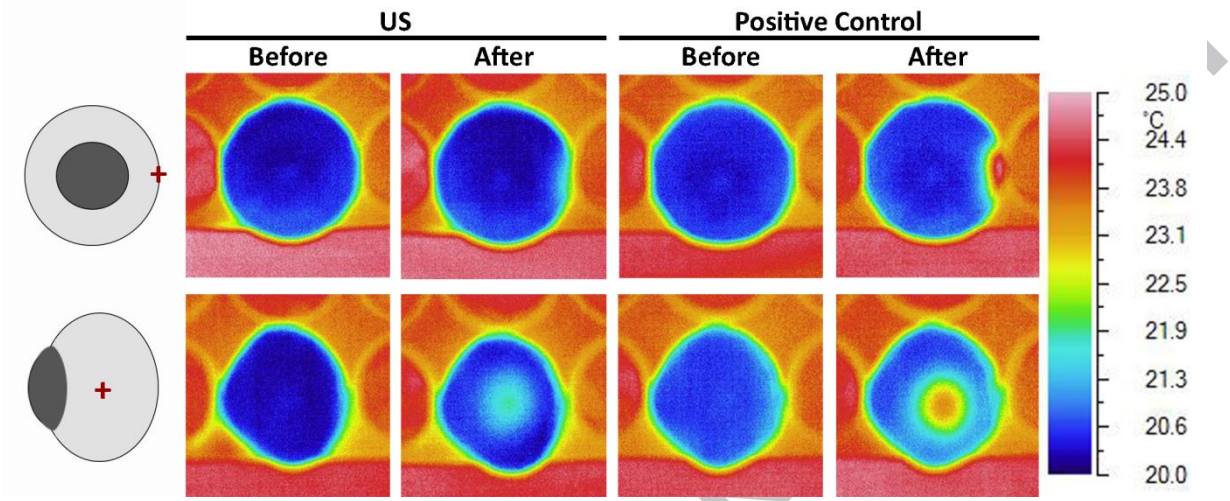

Fig. 10. Heat maps of *ex vivo* bovine eyes at room temperature before and after US application. Red crosses mark the site of US application.

Since tissue damage generally depends on the US parameters [36], short duration and low frequency US (1 MHz, 0.5 W/cm^2, 30 s) was employed in the present study due to potential safety concerns of higher frequencies and longer durations. A maximal allowed mechanical index (a metric of the non-thermal damage caused by US) of 0.23 and a thermal index of 1.0 for US application in ophthalmology have been set by the U.S. Food and Drug Administration (FDA) and the American Institute of Ultrasound in Medicine, which are far below the levels applied in other organs [37]. In this study, the US energy output with current settings was relatively low and there were no significant structural alterations or a significant temperature rise in the *ex vivo* ocular tissues due to the induced low energy level. The US energy generated here was only about 12 J (0.5 W/cm^2 of acoustic intensity × 30 s of duration × 0.8 cm^2 of effective area), although the intensity of 0.5 W/cm^2 was over the FDA approved level of 17 mW/cm^2 for diagnostic application in ophthalmology [38]. Future studies should further optimize the US parameters and evaluate the safety of long-term US application *in vivo* performing functional tests such as electroretinography. Moreover, it would be useful to design an US device specifically for ocular drug delivery that is fitted to the curvature of the eye ball.

4. Conclusion

This study investigated a novel method for ocular drug delivery by combining nanocarriers with US application, allowing for enhanced and sustained drug delivery to the retina to achieve a more prolonged clinical effect. Compared to passive diffusion of NPs, short-time US application increased the retinal penetration of HA coated NPs. The effect of US-enhanced permeation was transient with

repeated US application exhibiting a more significant effect than single treatment. Furthermore, US improved the mobility of NPs through the vitreous with current US conditions not causing any detectable damage to the ocular tissues. Overall, this work showed for the first time that transscleral US could be a powerful and safe tool to enhance retinal delivery with the combination of nanocarriers and US application holding great promise for efficient retinal drug delivery after intravitreal injection.

Conflicts of interest

The authors report no conflict of interest.

Acknowledgements

The authors would like to thank the Health Research Council of New Zealand [14/018] and the Buchanan Charitable Foundation for their financial support.

References

[1] P. Bishop, The biochemical structure of mammalian vitreous, Eye, 10 (1996) 664-670.

[2] A. Laude, L.E. Tan, C.G. Wilson, G. Lascaratos, M. Elashry, T. Aslam, N. Patton, B. Dhillon, Intravitreal therapy for neovascular age-related macular degeneration and inter-individual variations in vitreous pharmacokinetics, Prog. Retin. Eye Res., 29 (2010) 466-475.

[3] M. El Sanharawi, L. Kowalczuk, E. Touchard, S. Omri, Y. de Kozak, F. Behar-Cohen, Protein delivery for retinal diseases: from basic considerations to clinical applications, Prog. Retin. Eye Res., 29 (2010) 443-465.

[4] R.D. Jager, L.P. Aiello, S.C. Patel, E.T. Cunningham, Jr., Risks of intravitreous injection: a comprehensive review, Retina, 24 (2004) 676-698.

[5] S.K. Sahoo, F. Dilnawaz, S. Krishnakumar, Nanotechnology in ocular drug delivery, Drug Discov. Today, 13 (2008) 144-151.

[6] Y. Lu, N. Zhou, X. Huang, J.W. Cheng, F.Q. Li, R.L. Wei, J.P. Cai, Effect of intravitreal injection of bevacizumab-chitosan nanoparticles on retina of diabetic rats, Int. J. Ophthalmol., 7 (2014) 1-7.

[7] Y.S. Chen, C.R. Green, K.L. Wang, H.V. Danesh-Meyer, I.D. Rupenthal, Sustained intravitreal delivery of connexin43 mimetic peptide by poly(D,L-lactide-co-glycolide) acid micro- and nanoparticles - Closing the gap in retinal ischaemia, Eur. J. Pharm. Biopharm., 95 (2015) 378-386.

[8] W.L. Suen, Y. Chau, Specific uptake of folate-decorated triamcinolone-encapsulating nanoparticles by retinal pigment epithelium cells enhances and prolongs antiangiogenic activity, J. Control. Release, 167 (2013) 21-28.

[9] M. Murata, S. Horiuchi, Hyaluronan synthases, hyaluronan and its CD44 receptors in the posterior segment of rabbit eye, Ophthalmologica, 219 (2005) 287-291.

[10] L. Gan, J. Wang, Y. Zhao, D. Chen, C. Zhu, J. Liu, Y. Gan, Hyaluronan-modified core-shell liponanoparticles targeting CD44-positive retinal pigment epithelium cells via intravitreal injection, Biomaterials, 34 (2013) 5978-5987.

[11] T.F. Martens, K. Remaut, H. Deschout, J.F. Engbersen, W.E. Hennink, M.J. van Steenbergen, J. Demeester, S.C. De Smedt, K. Braeckmans, Coating nanocarriers with hyaluronic acid facilitates intravitreal drug delivery for retinal gene therapy, J. Control. Release, 202 (2015) 83-92.

[12] V. Zderic, S. Vaezy, R.W. Martin, J.I. Clark, Ocular drug delivery using 20-kHz ultrasound, Ultras. Med. Biol., 28 (2002) 823-829.

[13] W.L. Suen, H.S. Wong, Y. Yu, L.C. Lau, A.C. Lo, Y. Chau, Ultrasound-mediated transscleral delivery of macromolecules to the posterior segment of rabbit eye *in vivo*, Invest. Ophthalmol. Vis. Sci., 54 (2013) 4358-4365.

[14] L. Peeters, I. Lentacker, R.E. Vandenbroucke, B. Lucas, J. Demeester, N.N. Sanders, S.C. De Smedt, Can ultrasound solve the transport barrier of the neural retina?, Pharm. Res., 25 (2008) 2657-2665.

[15] H.V. Danesh-Meyer, N.M. Kerr, J. Zhang, E.K. Eady, S.J. O'Carroll, L.F. Nicholson, C.S. Johnson, C.R. Green, Connexin43 mimetic peptide reduces vascular leak and retinal ganglion cell death following retinal ischaemia, Brain, 135 (2012) 506-520.

[16] D. Huang, Y.S. Chen, I.D. Rupenthal, Hyaluronic acid coated albumin nanoparticles for targeted peptide delivery to the retina, Mol. Pharm., 14 (2017) 533-545.

[17] N. Yerushalmi, R. Margalit, Hyaluronic acid-modified bioadhesive liposomes as local drug depots: Effects of cellular and fluid dynamics on liposome retention at target sites, Arch. Biochem. Biophys., 349 (1998) 21-26.

[18] L. Pitkanen, J. Pelkonen, M. Ruponen, S. Ronkko, A. Urtti, Neural retina limits the nonviral gene transfer to retinal pigment epithelium in an in vitro bovine eye model, AAPS J., 6 (2004) 72-80.

[19] Q. Xu, N.J. Boylan, J.S. Suk, Y.Y. Wang, E.A. Nance, J.C. Yang, P.J. McDonnell, R.A. Cone, E.J. Duh, J. Hanes, Nanoparticle diffusion in, and microrheology of, the bovine vitreous ex vivo, J. Control. Release, 167 (2013) 76-84.

[20] T.F. Martens, D. Vercauteren, K. Forier, H. Deschout, K. Remaut, R. Paesen, M. Ameloot, J.F. Engbersen, J. Demeester, S.C. De Smedt, K. Braeckmans, Measuring the intravitreal mobility of nanomedicines with single-particle tracking microscopy, Nanomedicine, 8 (2013) 1955-1968.

[21] M. Yu, S. Jambhrunkar, P. Thorn, J. Chen, W. Gu, C. Yu, Hyaluronic acid modified mesoporous silica nanoparticles for targeted drug delivery to CD44-overexpressing cancer cells, Nanoscale, 5 (2013) 178-183.

[22] R. Farjo, J. Skaggs, A.B. Quiambao, M.J. Cooper, M.I. Naash, Efficient non-viral ocular gene transfer with compacted DNA nanoparticles, PLoS One, 1 (2006) e38.

[23] M. Nabili, H. Patel, S.P. Mahesh, J. Liu, C. Geist, V. Zderic, Ultrasound-enhanced delivery of antibiotics and anti-inflammatory drugs into the eye, Ultras. Med. Biol., 39 (2013) 638-646.

[24] V. Zderic, J.I. Clark, S. Vaezy, Drug delivery into the eye with the use of ultrasound, J. Ultras. Med., 23 (2004) 1349-1359.

[25] A. Razavi, D. Clement, R.A. Fowler, A. Birer, F. Chavrier, J.L. Mestas, F. Romano, J.Y. Chapelon, A. Begle, C. Lafon, Contribution of inertial cavitation in the enhancement of *in vitro* transscleral drug delivery, Ultras. Med. Biol., 40 (2014) 1216-1227.

[26] G. Merino, Y.N. Kalia, R.H. Guy, Ultrasound-enhanced transdermal transport, J. Pharm. Sci., 92 (2003) 1125-1137.

[27] A.C. Cheung, Y. Yu, D. Tay, H.S. Wong, R. Ellis-Behnke, Y. Chau, Ultrasound-enhanced intrascleral delivery of protein, Int. J. Pharm., 401 (2010) 16-24.

[28] J. Collis, R. Manasseh, P. Liovic, P. Tho, A. Ooi, K. Petkovic-Duran, Y. Zhu, Cavitation microstreaming and stress fields created by microbubbles, Ultrasonics, 50 (2010) 273-279.

[29] A. Sud, S. Dindyal, Microbubble therapies, INTECH Open Access Publisher, 2012.

[30] S. Sonoda, K. Tachibana, T. Yamashita, M. Shirasawa, H. Terasaki, E. Uchino, R. Suzuki, K. Maruyama, T. Sakamoto, Selective gene transfer to the retina using intravitreal ultrasound irradiation, J. Ophthalmol., 2012 (2012) 1-5.

[31] M. Lafond, F. Aptel, J.L. Mestas, C. Lafon, Ultrasound-mediated ocular delivery of therapeutic agents: a review, Expert Opin. Drug Deliv., (2016) 1-12.

[32] J. Sebag, K. Yee, Vitreous: from biochemistry to clinical relevance, in: Duane's foundations of clinical ophthalmology, Lippincott Williams & Wilkins, Philadelphia, 1998.

[33] J. Xu, J.J. Heys, V.H. Barocas, T.W. Randolph, Permeability and diffusion in vitreous humor: implications for drug delivery, Pharm. Res., 17 (2000) 664-669.

[34] J. Park, P.M. Bungay, R.J. Lutz, J.J. Augsburger, R.W. Millard, A. Sinha Roy, R.K. Banerjee, Evaluation of coupled convective-diffusive transport of drugs administered by intravitreal injection and controlled release implant, J. Control. Release, 105 (2005) 279-295.

[35] L.C. Junqueira, G. Bignolas, R.R. Brentani, Picrosirius staining plus polarization microscopy, a specific method for collagen detection in tissue sections, Histochem. J., 11 (1979) 447-455.

[36] M.R. Bohmer, C.H. Chlon, B.I. Raju, C.T. Chin, T. Shevchenko, A.L. Klibanov, Focused ultrasound and microbubbles for enhanced extravasation, J. Control. Release., 148 (2010) 18-24.

[37] U.S. FDA, Information for manufacturers seeking marketing clearance of diagnostic ultrasound systems and transducers, in, Center for Devices and Radiological Health, U.S. Department of Health and Human Services, Food and Drug Administration, 1997.

[38] K.H. Ng, International guidelines and regulations for the safe use of diagnostic ultrasound in medicine, J. Ultras. Med., 10 (2002) 5-9.